Toxicology in Vitro 66 (2020) 104835

Contents lists available at ScienceDirect

Toxicology in Vitro

journal homepage: www.elsevier.com/locate/toxinvit

Bioavailability of hydrophobic organic chemicals on an in vitro metabolic transformation using rat liver S9 fraction

Jung-Hwan Kwon[a,*], Hyun-Jeoung Lee[a,b], Beate I. Escher[c,d]

[a] Division of Environmental Science and Ecological Engineering, Korea University, 145 Anam-ro, Seongbuk-gu, Seoul 02841, Republic of Korea
[b] National Institute of Environmental Research, Environmental Research complex, 42 Hwangyeong-ro, Seo-gu, Incheon 22689, Republic of Korea
[c] Department of Cell Toxicology, Helmholtz Centre for Environmental Research – UFZ, Permoserstr. 15, DE-04318 Leipzig, Germany
[d] Environmental Toxicology, Center for Applied Geoscience, Eberhard Karls University Tübingen, Hölderlinstr. 12, DE-72074 Tübingen, Germany

ARTICLE INFO

Keywords:
Enzyme kinetics
Facilitated transport
Non-specific sorption
Equilibrium binding constants
In vitro-in vivo extrapolation (IVIVE)

ABSTRACT

Metabolic transformation of highly hydrophobic organic chemicals (HOCs) is one of the most important factors modulating their persistence, bioaccumulation and toxicity. Although sorption of HOCs to cellular matrices affects their bioavailability, it is still not clear how the cellular binding or sorption of HOCs in in vitro metabolism assays influences their enzymatic transformation kinetics. To elucidate effects of non-specific binding to enzymes, we measured apparent enzyme kinetics in an in vitro assay using four polycyclic aromatic hydrocarbons (phenanthrene, anthracene, pyrene and benzo[*a*]pyrene) as model HOCs and S9 mixture isolated from rat liver as a model enzyme mixture. The effects were also investigated in the presence of bovine serum albumin (BSA), which served to isolate the effect of protein binding from transformation. The observed transformation rates were much higher than those predicted assuming that only freely dissolved HOCs are available for metabolism. A new model including kinetic exchanges between non-specifically bound HOCs and those bound to active enzyme binding sites explained the apparent transformation kinetics at various experimental conditions better. The results are relevant for in vitro-in vivo extrapolation because the metabolic transformation rate in vivo may depend strongly on the local enzyme density and the micro-cellular environment. While non-specific protein binding reduces the unbound fraction of chemicals, this effect could be partially compensated by the facilitated transport to the active sites of the enzymes.

1. Introduction

Enzymatic transformation of hydrophobic organic chemicals (HOCs) has been of significant interest because their environmental persistence, bioaccumulation potential, and toxicity strongly depend on their metabolic transformation rate (Cowan-Ellsberry et al., 2008; Lee et al., 2019; Lo et al., 2016; Nichols et al., 2006). The increasing need to evaluate how fast HOCs undergo metabolic transformation cannot be met solely by in vivo tests because of long experimental time, high experimental cost and ethical concerns. High-throughput in vitro assays are therefore accepted as alternatives and complementary to in vivo testing and they come at various levels of complexity to evaluate potential for enzymatic transformation (Austin et al., 2002; Connors et al., 2013; Cowan-Ellsberry et al., 2008; Han et al., 2007; Jones and Houston, 2004; Kleinow et al., 1998; Lee et al., 2019; Lo et al., 2015). The simplest method among them is to measure the depletion of a parent chemical in the presence of microsomes or S9 mixture isolated from liver homogenate (Austin et al., 2002; Cowan-Ellsberry et al., 2008; Lee et al., 2019; Saunders et al., 2019).

In an enzymatic assay, the assay medium contains high density of proteins and other cellular materials. It is well-known that hydrophobic chemicals are strongly bound to cellular matrices and this sorption may affect their bioavailability (Austin et al., 2002; Fischer et al., 2019; Gülden and Seibert, 2005; Heringa et al., 2004; Hestermann et al., 2000; Kwon et al., 2007a). Reduced bioavailability of HOCs in such systems is often explained by the equilibrium sorption to medium and non-target sites, which makes them unavailable for the receptors in the test system. For example, Heringa et al. (2004) showed that serum protein concentration strongly influences dose-response relationship in an estrogenicity reporter gene assay and the effect concentrations should be normalized to free concentrations of hydrophobic estrogenic chemicals. Recent studies have confirmed this observation for a wide range of chemicals using a combined modeling and measurement approach (Escher et al., 2019; Fischer et al., 2017; Henneberger et al.,

* Corresponding author.
E-mail address: junghwankwon@korea.ac.kr (J.-H. Kwon).

https://doi.org/10.1016/j.tiv.2020.104835
Received 29 November 2019; Received in revised form 7 March 2020; Accepted 22 March 2020
Available online 26 March 2020
0887-2333/ © 2020 Published by Elsevier Ltd.

2019). Similarly, Austin and co-workers have shown that metabolic transformation rate is approximately constant if corrected for the extent of non-specific binding although the apparent transformation rate normalized to protein concentration decreases with increasing enzyme concentration (Austin et al., 2002, 2005). However, their work was limited to mostly ionizable pharmaceuticals of which the logarithms of ionization-corrected distribution ratios between 1-octanol and water at pH 7.4 (log $D_{7.4}$) were lower than 3.0.

On the contrary to the interpretation of decreased transformation rates caused by decrease in freely dissolved concentration, several studies noted that non-specific sorption might accelerate the transport of HOCs to the active target sites (Bittner et al., 2011; Blanchard et al., 2005; Bowman and Benet, 2018; Escher et al., 2011; Fujino et al., 2018; Kim et al., 2019; Matsunaga et al., 2019; Miyauchi et al., 2018; Poulin et al., 2016). Non-reactive proteins such as albumin are able to form substrate-albumin complexes and these complexes could deliver the substrate to the active target site. In vitro hepatic clearance rate was measured greater than expected with the decreased freely dissolved concentration in the extracellular medium especially for chemicals that strongly bind to albumin (Blanchard et al., 2005; Bowman and Benet, 2018; Kim et al., 2019; Poulin et al., 2016). Escher et al. (2011) compared bioconcentration factor (BCF) of HOCs in fish by extrapolating in vitro metabolic transformation rate obtained using S9 fraction isolated from rainbow trout (*Oncorhynchus mykiss*) with in vivo experimental values. The extrapolated BCF value for hydrophobic nonylphenol assuming that only freely dissolved fraction is available for metabolic transformation was much greater than the experimental BCF-values, suggesting a possibility of delivering nonylphenol non-specifically bound to proteins and other cellular matrices. However, the role of non-specific sorption of HOCs to the bioavailability in metabolic transformation is still not very clearly understood although this is crucial for extrapolating in vitro biotransformation studies to in vivo bioconcentration of highly HOCs.

In this study, we evaluated the effects of non-specific sorption on the apparent enzymatic kinetics in an in vitro metabolic transformation assay using four highly hydrophobic polycyclic aromatic hydrocarbons (PAHs), phenanthrene, anthracene, pyrene and benzo[*a*]pyrene, as model HOCs. Commercially available S9 mixture isolated from rat liver homogenate was chosen as the model enzyme mixture to provide a proof of principle. Apparent first-order transformation rate constants were measured at various S9 enzyme concentrations. Rate constants were also determined in the presence of various concentrations of bovine serum albumin (BSA) to evaluate facilitated transport of PAHs to S9 protein by BSA. In parallel, non-specific binding was measured in form of partition constants between S9 mixture and buffer and between BSA and buffer. A new enzyme kinetics model was proposed to explain the experimental data in this study.

2. Enzyme kinetic models

Enzymatic transformation of a substrate, *S*, can be described simply by model 1 in Fig. 1, where *E* is the enzyme, *E-S* is the enzyme-substrate complex after substrate binding to active enzyme sites, *P* is the product, and k_1, k_{-1}, k_2 are kinetic rate constants. Assuming irreversibility of metabolic transformation and pseudo-steady state of the formation of *E-S*, a simple rate expression well-known as Michaelis-Menten kinetics is obtained. Eq. (1) describes the rate of the total substrate depletion.

$$\text{rate} = -\frac{d[S]_T}{dt} = \frac{k_2[E]_T[S]_T}{\frac{k_{-1}+k_2}{k_1} + [S]_T} = \frac{V_{max}[E]_T[S]_T}{K_m + [S]} \tag{1}$$

where $[E]_T$ is the total concentration of the enzyme (mg L^{-1}), $[S]_T$ is the total substrate concentration (nmol L^{-1}), V_{max} is the maximum velocity (nmol mg^{-1} min^{-1}) and K_m is the half-saturation constant (nmol L^{-1}).

However, for HOCs, a large fraction of the substrate may be bound non-specifically to other protein sites than the active site (Austin et al., 2002; Heringa et al., 2004; Hestermann et al., 2000). Thus, the rate of formation of product is more likely to depend on freely dissolved substrate concentration $[S]_{free}$ than on the total concentration of substrate $[S]_T$ that is spiked in the assay medium due to non-specific binding to experimental matrices. Therefore, we may include non-specific binding in the kinetic model 2 as shown in Fig. 1. In general, non-specific sorption of hydrophobic chemicals between water and nano-sized cellular materials are known to be much faster than enzymatic transformation half-life (Cócera et al., 2001; Krause et al., 2018; Schlautman and Morgan, 1993). If we assume that equilibrium is obtained instantaneously, we can model the effects of non-specific sorption using the distribution constant between proteins and the solution. Free substrate concentration, $[S]_{free}$, can be estimated by assuming that $[E\text{-}S]$ is negligible (i.e., $[S]_T \cong [S]_{ns} + [S]_{free}$) compared to free and non-specifically sorbed substrates as:

$$[S]_{free} = \frac{[S]_T}{1 + K_{ns}[E]_T} \tag{2}$$

where K_{ns} is the distribution constant between protein and the buffer solution (L kg^{-1}) via non-specific sorption defined by Eq. (3).

$$K_{ns} = \frac{[S]_{ns}}{[E]_T[S]_{free}} \tag{3}$$

If total substrate concentration is sufficiently low (Eq. (4)),

$$\frac{k_{-1}+k_2}{k_1} \gg [S]_T \tag{4}$$

and only free substrates are available for metabolic transformation, Eq. (1) can be written as:

$$-\frac{d[S]_T}{dt} = \frac{k_1k_2}{k_{-1}+k_2} \cdot \frac{[E]_T}{1 + K_{ns}[E]_T}[S]_T \tag{5}$$

Thus, the apparent first-order rate constant would be expected to increase linearly with increasing enzyme concentration at sufficiently low $[E]_T$, then approach a constant value as $[E]_T$ increases (Eq. (6)).

$$k_{S9} = \frac{k_1k_2}{k_{-1}+k_2} \cdot \frac{[E]_T}{1 + K_{ns}[E]_T} \tag{6}$$

If we additionally assume that the non-specifically sorbed substrate can be delivered to the active site on the enzyme (Model 3 in Fig. 1), and describe this process with the rate constants, k_1' and k_{-1}', we obtain a modified rate expression as follows (see Section A, Electronic Supplementary Material for mathematical derivation):

$$-\frac{d[S]}{dt} = \frac{k_1k_2}{k_{-1}+k_{-1}'+k_2} \cdot \frac{\left(1 + \frac{k_1'}{k_1}K_{ns}[E]_T\right)[E]_T}{1 + K_{ns}[E]_T}[S]_T \tag{7}$$

There are two limiting cases of model 3. If the free fraction of substrate dominates (i.e., $K_{ns}[E]_T \ll 1$ and $k_1'K_{ns}[E]_T \ll k_1$) and the substrate concentration is much below the saturation level, Eq. (7) is simplified to:

$$-\frac{d[S]_T}{dt} = \frac{k_1k_2[E]_T}{k_{-1}+k_{-1}'+k_2}[S]_T \tag{8}$$

in which the pseudo-first order rate constant is proportional to the total enzyme concentration. On the other hand, if the bound forms dominate (i.e., $K_{ns}[E]_T \gg 1$ and $k_1'K_{ns}[E]_T \gg k_1$) and the substrate concentration is low enough, Eq. (5) is simplified to:

$$-\frac{d[S]_T}{dt} = \frac{k_1'k_2[E]_T}{k_{-1}+k_{-1}'+k_2}[S]_T \tag{9}$$

Eq. (9) is similar to Eq. (6) except for the slope. The ratio of the slope in Eq. (8) to that in Eq. (9) is equal to the ratio of association rate constants (i.e., $k_1$to k_1').

To test if the concept of non-specific sorption is applicable, we can

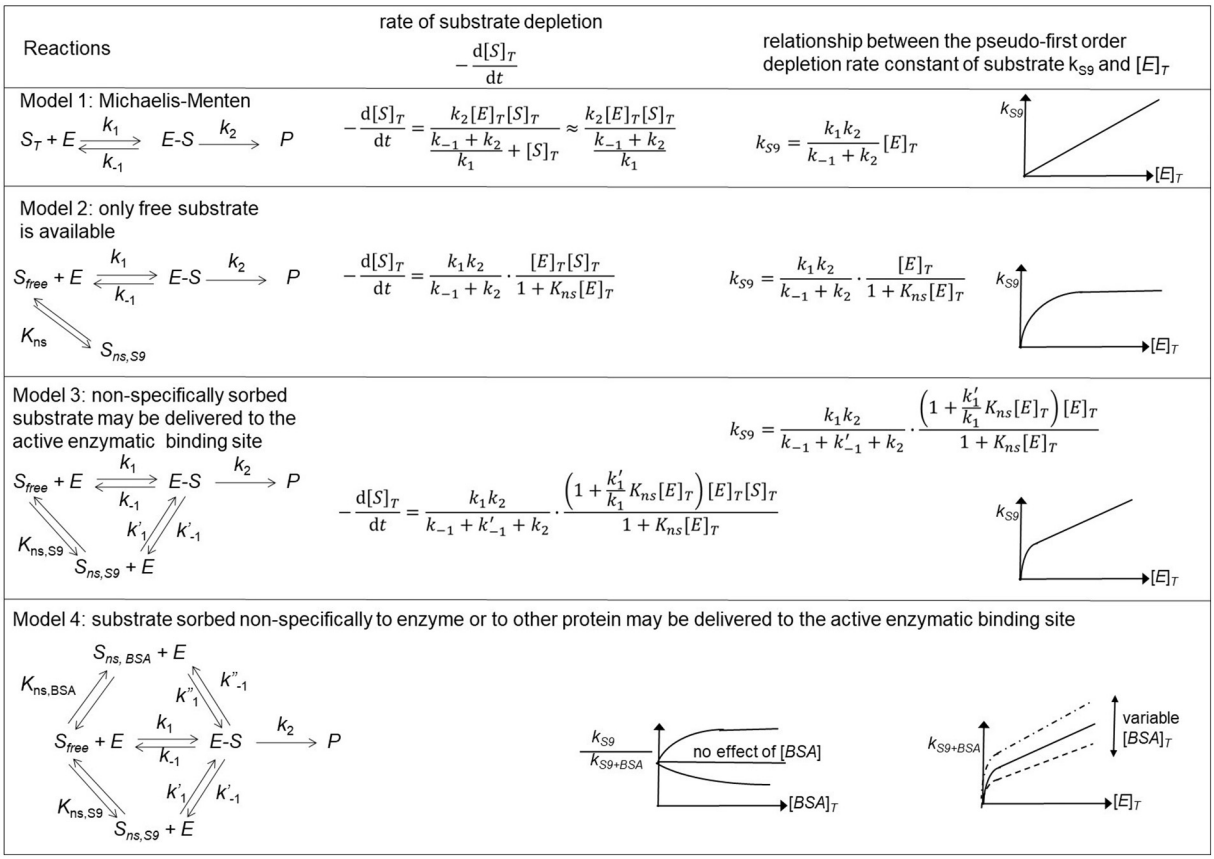

Fig. 1. Models describing enzymatic transformation kinetics: model 1, classical Michaelis-Menten model, applicable if the nominal concentration of substrate [S] is available; model 2 applicable if only free substrate $[S]_{free}$ are available; model 3, applicable if non-specifically sorbed substrate $[S]_{ns}$ may be delivered to the active enzymatic binding site; and model 4 applicable if there are other proteins (e.g., BSA) that can sorb substrate and the sorbed substrates may be delivered to the active binding site on S9 protein.

add a second, enzymatically inactive protein, bovine serum albumin (BSA). The reaction model implementing this additional process is depicted in Fig. 1 (model 4) but the kinetic equations are not solved.

We measured the transformation rate as a function of substrate concentration for a small number of controls to assure that $[S]_T << K_m$ (See Fig. 1, Supplementary Data). Under this condition it is possible to determine a pseudo-first order rate constant of substrate depletion (k_{S9}) which is equivalent to $V_{max}[E]_T/K_m$. Thus plotting k_{S9} versus $[E]_T$ will indicate which kinetic model describes the experimental data best (Fig. 1).

3. Materials and methods

3.1. Materials

Four polycyclic aromatic hydrocarbons (PAHs), phenanthrene (CAS RN 85–01-8, 98%, Aldrich, Buchs, Switzerland), anthracene (CAS RN 120–12-7, 99%, Fluka, Buchs, Switzerland), pyrene (CAS RN 129–00-0, 99%, Fluka), and benzo[*a*]pyrene (CAS RN 50–32-8, 99.9%, Supelco, Bellefonte, PA), were chosen as model hydrophobic compounds to evaluate their transformation kinetics in the presence of the enzyme mixture at various non-reactive protein concentrations. Hexachlorobenzene (CAS RN 118–74-1, > 99%, Fluka) was used as reference chemical in the sorption experiments because it is hardly degradable. Uninduced rat S9 mixture (Catalog no. RTS9-PL) was purchased from CellzDirect, Inc. (Austin, TX). The protein content of the S9 mixture from the supplier was used. Bovine serum albumin (BSA), dimethylsulfoxide (DMSO), NADP-sodium salts, glucose-6-phosphate, magnesium sulfate, and tris(hydroxymethyl)aminomethyl-chloride (Tris-HCl) were of high purity and purchased from Sigma-Aldrich, Inc. (St. Louis, MO).

3.2. Chemical analyses

Concentration of selected PAHs was analyzed using high-performance liquid chromatography system equipped with a P680 HPLC pump and an ASI-100 autosampler (Dionex Softron GmbH, Germering, Germany). They were separated on a C18 Supelcosil LC-PAH column (150 mm × 4.6 mm, 5 µm, Supelco, Bellefonte, PA) at 40 °C and detected using an RF-2000 fluorescence detector (Dionex). The excitation wavelength was 275 nm for phenanthrene, 260 nm for anthracene and pyrene, and 290 nm for benzo[*a*]pyrene and the emission wavelengths were 350 for phenanthrene, 420 nm for anthracene and pyrene, and 430 nm for benzo[*a*]pyrene. De-ionized water and acetonitrile were used as the mobile phase in isocratic mode with the flow rate of 1 mL min^{-1}.

3.3. Determination of partition constants and sorption constants

Partition constants between polydimethylsiloxane (PDMS) and 50 mM Tris buffer solution at pH 7.8 ($K_{PDMSbuffer}$) were determined using a dynamic permeation method (Kwon et al., 2007b). In short, $K_{PDMSbuffer}$ values were calculated from the apparent permeation rate constant from a PDMS disk loaded with chemicals to a clean PDMS disk separated by the buffer solution, k_d (s^{-1}), using the following relationship:

$$K_{PDMSbuffer} = \frac{D_{buffer}}{\delta_{buffer}} \frac{A}{V_{PDMS}} \frac{1}{k_d} \quad (10)$$

Table 1
Summary of partition constants between PDMS and Tris-buffer ($K_{PDMS/buffer}$), between S9 and buffer ($K_{S9/buffer}$) and between BSA and buffer ($K_{BSA/buffer}$) with literature log K_{ow}, log K_{PDMSw}, and log K_{lipw}.

Chemical	Partition constants						
	log K_{ow}	log K_{PDMSw}	log K_{lipw}	log $K_{PDMS/buffer}$	log $K_{S9(denatured)/buffer}$	log $K_{BSA(native)/buffer}$	log $K_{BSA(denatured)/buffer}$
Phenanthrene	4.52[a]	3.87 (3.77, 3.96)[b]	4.86[c], 5.07[d]	3.69 (3.57, 3.78)	4.38 (4.23, 4.49)	3.20 (3.00, 3.33)	3.09 (2.80, 3.33)
Anthracene	4.50[a]	3.98 (3.88, 4.06)[b]	5.15[d]	3.82 (3.72, 3.91)	4.57 (4.43, 4.68)	3.33 (3.21, 3.43)	3.30 (2.98, 3.27)
Pyrene	5.00[a]	4.36 (4.26, 4.45)[b]	5.78[d]	4.13 (3.97, 4.25)	4.87 (4.61, 5.03)	3.85 (3.66, 3.98)	3.59 (3.31, 3.37)
Benzo[*a*]pyrene	6.35[a]	5.09 (4.98, 5.18)[b]	6.98[c], 7.41[d]	5.01 (4.90, 5.09)	5.88 (5.63, 6.04)	4.49 (4.32, 4.61)	4.50 (4.26, 4.65)

Values in parenthesis are the lower and the upper 95% confidence limits calculated using error propagation.
[a] Values of log K_{ow} are recommended values in Sangster (1989).
[b] Values are from Kwon et al. (2007b).
[c] Values are from Kwon et al. (2009).
[d] Values are from Jonker and van der Heijden (2007) using SPME method.

where D_{buffer} is the diffusion coefficient of a chemical in the buffer solution ($m^2\ s^{-1}$), δ_{buffer} is the aqueous boundary layer thickness in the buffer solution (estimated to be 12.5 μm in a previous study; Kwon et al., 2007b), A is the surface area of the PDMS disk (m^2), V_{PDMS} is the volume of the PDMS disk (m^3), and k_d is the experimentally measured rate constant (s^{-1}). D_{buffer} was assumed to be equal to the aqueous diffusion coefficient estimated using a correlation with solute's molecular weight (Kwon et al., 2007b).

The sorption constants between buffer solution and denatured S9, native BSA or denatured BSA were measured using a PDMS depletion method (Escher et al., 2011; Kwon et al., 2009; Ter Laak et al., 2005). Rat S9 protein and BSA were denatured by increasing the pH of the solution using the equivalent volume of NaOH (yields pH of 14), then immersing the vials for 5 min in boiling water, followed by adjusting pH to 9.0 using concentrated HCl. In this way the precipitation of the denatured protein could be avoided.

The detailed procedures of measuring partition constants and sorption constants were described previously (Kwon et al., 2007b, 2009). PDMS disks loaded with chemical species were depleted in the presence of various volumes of deactivated S9 or BSA solution. Partition constants $K_{PDM/Ssus}$ were obtained using a non-linear regression between the fraction lost to the suspension ($C_{PDMS}/C_{PDMS,0}$) and the volume ratio V_{sus}/V_{PDMS} ($m^3_{suspension}\ m^{-3}_{PDMS}$):

$$\frac{C_{PDMS}}{C_{PDMS,0}} = \frac{1}{1 + \frac{V_{sus}/V_{PDMS}}{K_{PDMS/sus}}} \tag{11}$$

where C_{PDMS} is the concentration of a chemical in PDMS after equilibrium (mol m^{-3}), $C_{PDMS,0}$ is the initial concentration in PDMS (mol m^{-3}), $K_{PDM/Ssus}$ is the partition constant between PDMS and the suspension containing S9 or BSA ($m^3_{suspension}\ m^{-3}_{PDMS}$). Then, the partition constant between protein and buffer ($K_{protein/buffer}$, L kg^{-1}) wss calculated by

$$K_{protein/buffer} = \frac{\frac{K_{PDMS/buffer}}{K_{PDMS/sus}} - 1}{m_{protein}} \tag{12}$$

where $K_{PDMSbuffer}$ is the partition constant between PDMS and buffer and $m_{protein}$ is protein concentration in the suspension (kg L^{-1}). These partition constants were used to quantitatively describe non-specific binding (or sorption) in the metabolic transformation assay.

3.4. In vitro metabolic transformation assay

Apparent transformation rate constants were measured at various S9 enzyme concentrations. 8 μL of dimethylsulfoxide containing the test chemical was spiked into an amber vial containing 10 mM NaNADP, 10 mM $MgCl_2$, 40 mM glucose-6-phosphate, and desired concentration of S9 and BSA in 50 mM Tris buffer (pH 7.8) to make a total volume of 1600 μL. The initial concentration of selected PAHs was approximately 100 nM, which is low enough to fall into the linear range of Michaelis-Menten kinetics based on published half-saturation constants of PAHs (Fitzsimmons et al., 2001) and confirmed by the screening experiments in the presented set-up (Fig. S1, Electronic Supplementary Material). The enzymatic transformation experiments were conducted at 25 °C in the dark because all partition constants were measured at this temperature and the purpose of this study was to provide a proof of principle. The solution was shaken gently at 90 rpm. After pre-determined incubation time (up to 2 h), 200 μL of the solution was taken and immediately mixed with 1800 μL ice-cold acetonitrile to quench the enzymatic transformation. The mixture was then centrifuged at 3000*g* for 10 min to precipitate proteins and the supernatant was taken for chemical analysis. The pseudo-first order transformation rate constant k_{S9} was obtained using linear regression (Eq. (11)) using concentration measured at six different time points.

$$ln\frac{[S]}{[S_0]} = -k_{S9}t \tag{13}$$

For a control experiment, changes in concentration of PAHs were also measured in the presence of denatured S9.

4. Results

4.1. Partition constants between S9 and buffer and between BSA and buffer

Table 1 shows all partition and sorption constants obtained in this study and a comparison of the data with octanol-water partition constants (K_{ow}), PDMS-water partition constants (K_{PDMSw}), and liposome-water partition constants (K_{lipw}) using palmitoyl-oleoyl-phosphatidylcholine from literature (Jonker and van der Heijden, 2007).

Values of $K_{PDMSbuffer}$ were $10^{3.69}$, $10^{3.82}$, $10^{4.13}$, and $10^{5.01}$ for phenanthrene, anthracene, pyrene, and benzo[*a*]pyrene, respectively, as shown in Table 1 (see Fig. S2, Electronic Supplementary Material for experimental determination of the mass transfer kinetics). The values of $K_{PDMS/buffer}$ resulting from a fit of the experimentally measured rate constants were slightly but not statistically significantly smaller than K_{PDMSw} obtained using de-ionized water (Kwon et al., 2007b).

Table 1 also shows $K_{S9/buffer}$, $K_{BSA(native)/buffer}$ and $K_{BSA(denatured)/buffer}$ values obtained using Eq. (12) after determining $K_{PDMSsus}$ using non-linear regression (Eq. (11)) of the fraction remaining in PDMS ($C_{PDMS}/C_{PDMS,0}$) versus volume ratio (see Fig. S3, Electronic Supplementary Material). $K_{BSA(native)/buffer}$ and $K_{BSA(denatured)/buffer}$ agreed well, indicating that the assumption is justified that non-specific binding of HOCs to proteins can be regarded as a partitioning process. Control experiments with hexachlorobenzene, which is not metabolizable, also indicated that sorption is not only independent of the tertiary structure of BSA but also independent of the tertiary structure of the S9, because there was no difference between $K_{S9(native)/buffer}$ and $K_{S9(denatured)/buffer}$ (see Fig. S4, Electronic Supplementary Material) and pH changes prior

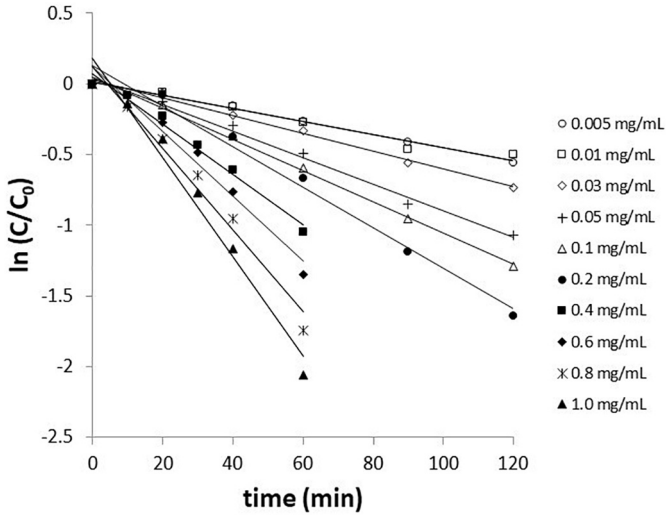

Fig. 2. Determination of pseudo-first order rate constant at various S9 concentration for benzo[*a*]pyrene as an example. C and C_0 stand for the total substrate concentration at time t and $t = 0$.

and after the denaturation affected the results only slightly. $K_{BSA(native)/buffer}$ values were lower than K_{ow} values by a factor of 14 (pyrene) to 72 (benzo[*a*]pyrene). This difference is in a good agreement with a compilation of data showing that protein-water partition constants are lower than K_{ow} by approximately a factor of 20 (de Bruyn and Gobas, 2007).

4.2. Effects of enzyme concentration on the metabolic rate

Concentration of PAHs remained unchanged in the presence of denatured S9. The transformation in presence of native S9 followed first-order reaction kinetics with r^2 values mostly higher than 0.9. Fig. 2 shows an example of pseudo-first order kinetic decay for benzo[*a*]pyrene at various S9 concentrations. Fig. 3 shows the pseudo-first order substrate depletion rate constants k_{S9} (min^{-1}) at various S9 enzyme concentrations for the selected PAHs compiled from at least three different independent experiments. There were detectable rate constants even at very low S9 concentration (0.025–0.05 $mg_{protein}$ mL^{-1}). There was a steep increase in the rate constant followed by a gradual linear increase with increasing enzyme concentration. Dashed and solid lines in Fig. 3 denote best-fit lines for model 2 and 3 (Eqs. (5) and (7)), respectively, using the experimentally measured $K_{S9/buffer}$ values as K_{ns} values.

A linear relationship between the apparent rate constant and the total enzyme concentration would be expected according to the classical Michaelis-Menten kinetics (model 1) and the saturation of the apparent rate constant would be expected with increase of the total enzyme concentration according to model 2 but neither model can explain the experimental data. The experimental bi-phasic increase in the apparent rate constant is best explained by model 3 that assumes that non-specifically bound HOCs are also available for enzymatic transformation. The initial steep increase followed by a steady increase in the apparent rate constant indicates that freely dissolved PAHs are more readily available for enzymatic transformation but PAHs non-specifically bound to S9 and cellular matrices are also bioavailable and cannot be neglected although their contribution is slower, so they are not fully available. This means for Eq. (5) that k_1 is much higher than k_1' but k_1' is sufficiently greater than zero to affect the apparent transformation kinetics.

4.3. Effects of variable BSA concentrations

We also tested if additional non-specific binding has the same effect as S9 by running experiments with mixtures of 0.5 mg mL^{-1} S9 with different BSA concentrations (0 to 5 mg mL^{-1}). Fig. 4 shows apparent first-order rate constants k_{S9+BSA} normalized by the rate constant without BSA, k_{S9}. These ratios k_{S9+BSA}/k_{S9} decreased with increasing BSA for phenanthrene, anthracene, and pyrene (Fig. 4a, b, and c). However, the opposite trend was observed for benzo[*a*]pyrene (Fig. 4d). Dashed lines refer to predicted ratios k_{S9+BSA}/k_{S9} with using $K_{BSA/buffer}$ and $K_{S9/buffer}$ under the assumption that non-specific sorption to BSA makes the substrate unavailable for enzymatic transformation and distribution of species in the assay medium is near equilibrium (model 2). The decrease in the freely dissolved concentration by adding BSA to the system satisfactorily explained the decreased apparent rate constants for phenanthrene, anthracene and pyrene although data scattered, whereas this hypothesis fails to explain the experimental data of benzo[*a*]pyrene.

5. Discussion

5.1. Non-specific sorption of PAHs to S9 and BSA

As summarized in Table 1, $K_{BSA(native)/buffer}$ and $K_{BSA(denatured)/buffer}$ agreed well, indicating that sorption of HOCs to proteins could be regarded as non-specific partitioning. Losing the tertiary structure of the protein through denaturation does not seem to affect the partitioning. Negligible differences between $K_{S9(native)/buffer}$ and $K_{S9(denatured)/buffer}$ for the positive control using non-degradable hexachlorobenzene also supports that this non-specific sorption is independent on the tertiary structure of BSA or S9 and the solution pH (Fig. S4). This finding is important because it confirms that the $K_{S9/buffer}$ values, which need to be determined with denatured S9 to differentiate binding from transformation, are representative for native S9. In addition, log $K_{BSA/buffer}$ increased with increasing log K_{ow} (Table 1), suggesting that the affinity of PAHs to albumin is rather unchanged, but the decrease in their aqueous solubility increases log $K_{BSA/buffer}$.

It is also interesting that the experimentally determined $K_{S9/buffer}$ values were higher than $K_{BSA/buffer}$ by approximately one order of magnitude (Table 1). Although protein content of the commercial S9 mixture used in this study was quantified and all results were expressed in relation to protein content of the S9, there was no information on the amount of residual lipids. Liposome-water partition constants (K_{lipw}) of the selected PAHs using palmitoyl-oleoyl-phosphatidylcholine were slightly higher than their K_{ow} values (Jonker and van der Heijden, 2007; Kwon et al., 2009) as shown in Table 1. Thus, only 5–10% of residual lipid (w/w) may result in the extraordinarily high sorption constant due to dominating contribution of residual lipids. For comparison, fetal bovine serum contains 2.9% lipids ($m_{lip}/(m_{lip} + m_{protein})$ (Fischer et al., 2017) and it is conceivable that S9 has a similar lipid content. In contrast the commercially available BSA is purified and fatty acid-free. Although further validation is needed to rationalize the unusually high non-specific sorption to S9 proteins, these sorption constants can be used for the purpose of evaluation of bioavailability of highly HOCs in S9 enzymatic transformation assay.

5.2. Comparison of enzyme kinetic models

As shown in Fig. 3, the apparent enzymatic transformation rate constants for the four PAHs followed model 3, indicating that HOCs non-specifically sorbed to non-active site of S9 proteins and other organic matter such as proteins and lipids in the medium are still available for enzymatic transformation although they are not as promptly available as freely dissolved forms. This trend in Fig. 3, however, does not agree with a recent biotransformation study for phenanthrene, pyrene, and benzo[*a*]pyrene with liver S9 fractions isolated from rainbow trout (Nichols et al., 2018). Although it needs further investigations, this conflict might be due to (1) differences between S9 enzymes used, (2) potential roles of other components such as lipids in

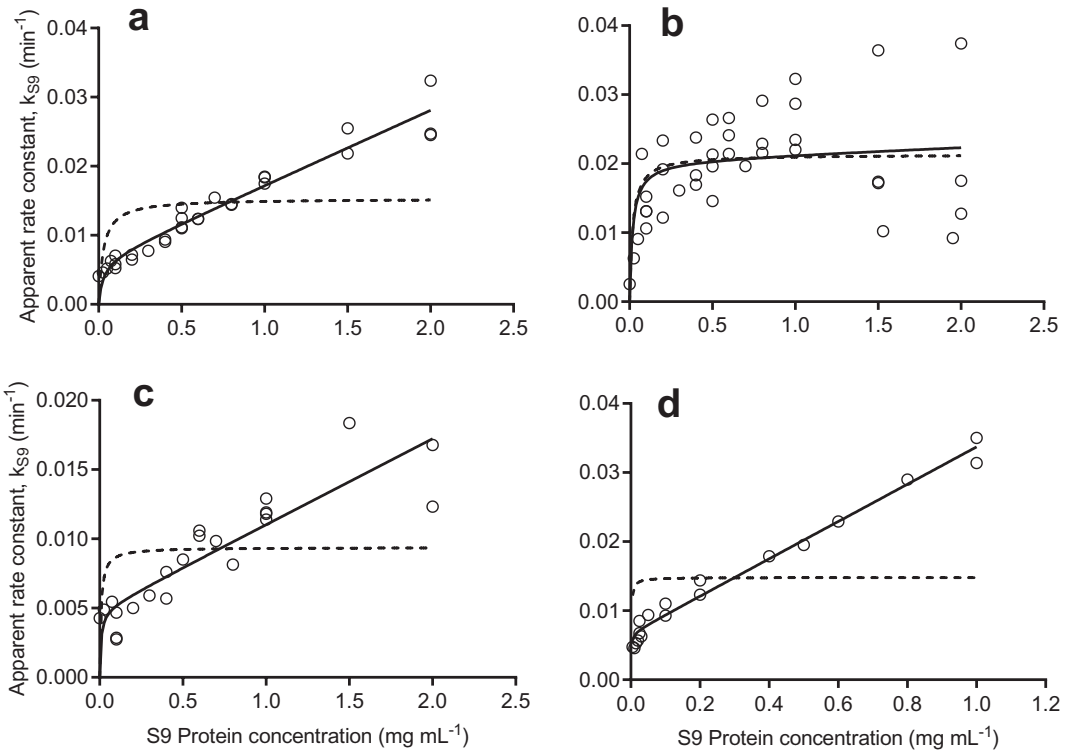

Fig. 3. Apparent first-order rate constant k_{S9} at various enzyme concentrations for (a) phenanthrene, (b) anthracene, (c) pyrene, and (d) benzo[*a*]pyrene. The solid lines illustrate the best-fit curves using the new model (Eq. (7)) with the best-fit parameters given in the Electronic Supplementary Material (Table S1). For comparison, the dashed lines show the model that assumed that only free substrates are available (Eq. (6)).

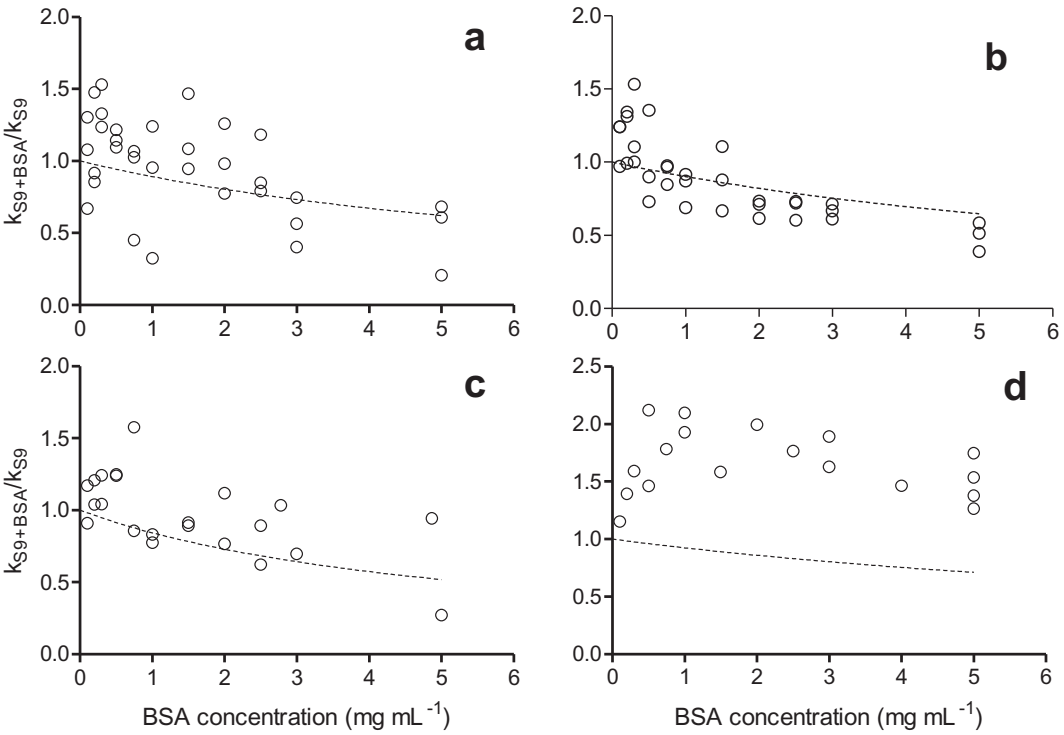

Fig. 4. Apparent relative first-order rate constant in the presence of bovine serum albumin k_{S9+BSA}/ k_{S9} for (a) phenanthrene, (b) anthracene, (c) pyrene, and (d) benzo[*a*]pyrene. The concentration of S9 mixture was 0.5 mg mL^{-1}. Dashed lines illustrate expected curves if only free substrate $[S]_{free}$ is available for enzymatic transformation (model 2 in Fig. 1).

S9 mixtures, and (3) lower incubation temperature (11 °C) and longer experimental time for rainbow trout S9.

The extension of the proposed kinetic model (model 4 in Fig. 1) provides a useful insight for the availability of HOCs to the enzymatic transformation in more complex and thus closer to in vivo conditions. If we assume that substrates non-specifically bound to non-reactive

proteins such as BSA are still available for enzymatic activation (i.e., forming [*E-S*] complex), we may introduce another association rate constant (k_1'') from sorbed to BSA to the active reaction site and dissociation rate constant (k_{-1}'') from the active site to sorbed to BSA. If k_1'' is negligibly small compared to k_1 or k_1', normalized rate constants would be close to that predicted by the model shown in Fig. 4. On the other hand, we may not neglect the effects of k_1'' in the overall enzymatic kinetics if k_1'' is not negligibly small. The experimental results of benzo[*a*]pyrene can be predicted if k_1'' is higher than k_1'. Thus, the observed enzymatic transformation kinetics may or may not decrease depending on the chemical investigated and its sorption behavior. Krause and Goss (2018a, 2018b) proposed in vitro-in vivo extrapolation models including desorption rate constants of HOCs from protein to explain how binding to proteins affect the overall hepatic clearance. Because hepatic metabolism depends on desorption rate constant, fraction bound to proteins, and the intrinsic metabolic rate constant by enzymes (Krause and Goss, 2018b), further investigation on enzymatic kinetics in the presence of various cellular matrices is required.

5.3. Implications for environmental bioconcentration of HOCs

Many highly HOCs are suspected to bioconcentrate in aquatic and terrestrial organisms and the key parameter that determines the BCF is in vivo clearance rate (Cowan-Ellsberry et al., 2008; Lee et al., 2019; Nichols et al., 2006). Experimental data in this study clearly showed that not only freely dissolved HOCs are available for metabolic transformation but also HOCs non-specifically bound to serum proteins or residual lipids are available, providing a clue why experimental BCF values for HOCs are often found to be greater than extrapolated using in vitro enzymatic transformation rate (Escher et al., 2011).

5.4. Implications for human quantitative in vitro to in vivo extrapolation models (QIVIVE)

The mechanistic model presented here for in vitro metabolism has also implications for the in vivo situation in human pharmacokinetic models, where it is difficult to estimate the quantitative contribution of non-specifically bound HOCs to be delivered to the active enzymatic sites. We performed the experiments at 25 °C for internal model consistency because the physicochemical parameters are mainly available at 25 °C. Temperature correction is possible but not needed for proof of concept. The concept should be easily transferable to lower temperatures (fish studies) and higher temperatures (mammalian studies).

Recent studies provided evidence of the facilitated transport of drugs by albumin-mediated cellular uptake mechanisms for the protein bound fraction in hepatocytes and cardiac myocytes (Bteich et al., 2019; Fujino et al., 2018; Kim et al., 2019; Matsunaga et al., 2019; Poulin et al., 2016). Albumin also enhanced oxidation activities of human liver microsomal cytochrome P450 enzymes (Shimura et al., 2019). This study was empirical and did not offer a mechanistic explanation but the result is consistent with changes in the enzymatic transformation rates with varying non-specific bindings to S9 and BSA in this study. Roles of albumin and other sub-cellular components on the enzymatic reaction rates in a sub-cellular environment warrant further investigations. Bteich et al. (2019) also recommended the also recommend inclusion of albumin-mediated uptake in IVIVE models for hepatic clearance and the proposed modeling framework provides one path. Since in vitro studies aim at an extrapolation to in vivo, results from in vitro study should be applied for prediction of fate in vivo with great care because the actual metabolic rate in vivo may also depend on local enzyme density and micro-cellular environment. The changes in the apparent transformation rate or the clearance rate should be assessed for more HOCs in the presence of diverse matrices in the microenvironment where the metabolic transformation takes place.

Declaration of Competing Interest

The authors declare that they have no known competing financial interests or personal relationships that could have appeared to influence the work reported in this paper.

Acknowledgments

Most of experiments of this study was conducted in 2007-2008 at Eawag, Switzerland, and was financially supported by 3R research foundation, Switzerland (3R-Project 100-06). We thank Sibylle Rutishauser (Eawag) for experimental assistance. We are grateful to the HESI Bioaccumulation Project Committee coordinated by Michelle Embry, Annie Weisbrod, Chris Cowan-Ellsberry, and Sue Erhardt for discussions and feedback.

Appendix A. Supplementary data

Supplementary data to this article can be found online at https://doi.org/10.1016/j.tiv.2020.104835.

References

Austin, R.P., Barton, P., Cockroft, S.L., Wenlock, M.C., Riley, R.J., 2002. The influence of nonspecific microsomal binding on apparent intrinsic clearance, and its prediction from physicochemical properties. Drug Metab. Dispos. 30, 1497–1503. https://doi.org/10.1124/dmd.30.12.1497.

Austin, R.P., Barton, P., Mohmed, S., Riley, R.J., 2005. The binding of drugs to hepatocytes and its relationship to physicochemical properties. Drug Metab. Dispos. 33, 419–425. https://doi.org/10.1124/dmd.104.002436.

Bittner, M., Macikova, P., Giesy, J.P., Hilscherova, K., 2011. Enhancement of AhR-mediated activity of selected pollutants and their mixtures after interaction with dissolved organic matter. Environ. Int. 37, 960–964. https://doi.org/10.1016/j.envint.2011.03.016.

Blanchard, N., Alexandre, E., Abadie, C., Lavé, T., Heyd, B., Mantion, G., Jaeck, D., Richert, L., Coassolo, P., 2005. Comparison of clearance predictions using primary cultures and suspensions of human hepatocytes. Xenobiotica 35, 1–15. https://doi.org/10.1080/00498250400021820.

Bowman, C.M., Benet, L.Z., 2018. An examination of protein binding and protein-facilitated uptake relating to in vitro-in vivo extrapolation. Eur. J. Pharm. Sci. 123, 502–514. https://doi.org/10.1016/j.ejps.2018.08.008.

Bteich, M., Poulin, P., Hadda, S., 2019. The potential protein-mediated hepatic uptake: discussion on the molecular interactions between albumin and the hepatocyte cell surface and their implications for the in vitro-in vivo extrapolations of hepatic clearance of drugs. Expert Opin. Drug Metab. Toxicol. 15, 633–658. https://doi.org/10.1080/17425255.2019.1640679.

Cócera, M., López, O., Estelrich, J., Parra, J.L., de la Maza, A., 2001. Use of a fluorescence spectroscopy technique to study the adsorption of sodium dodecylsulfonate on liposomes. Chem. Phys. Lipids 109, 29–36. https://doi.org/10.1016/s0009-3084(00)00205-x.

Connors, K.A., Du, B., Fitzsimmons, P.N., Hoffman, A.D., Chambliss, C.K., Nichols, J.W., Brooks, B.W., 2013. Comparative pharmaceutical metabolism by rainbow trout (*Oncorhynchus mykiss*) liver S9 fractions. Environ. Toxicol. Chem. 32, 1810–1818. https://doi.org/10.1002/etc.2240.

Cowan-Ellsberry, C.E., Dyer, S.D., Erhardt, S., Bernhard, M.J., Roe, A.L., Dowty, M.E., Weisbrod, A.V., 2008. Approach for extrapolating in vitro metabolism data to refine bioconcentration factor estimates. Chemosphere 70, 1804–1817. https://doi.org/10.1016/j.chemosphere.2007.08.030.

de Bruyn, A.M.H., Gobas, F.A.P.C., 2007. The sorptive capacity of animal protein. Environ. Toxicol. Chem. 26, 1803–1808. https://doi.org/10.1897/07-016R.1.

Escher, B.I., Cowan-Ellsberry, C.E., Dyer, S., Embry, M.R., Erhardt, S., Halder, M., Kwon, J.-H., Johanning, K., Oosterwijk, M.T.T., Rutishauser, S., Segner, H., Nichols, J., 2011. Protein and lipid binding parameters in rainbow trout (Oncorhynchus mykiss) blood and liver fractions to extrapolate from an in vitro metabolic degradation assay to in vivo bioaccumulation potential of hydrophobic organic chemicals. Chem. Res. Toxicol. 24, 1134–1143. https://doi.org/10.1021/tx200114y.

Escher, B.I., Glauch, L., König, M., Mayer, P., Schlichting, R., 2019. Baseline toxicity and volatility cut-off in reporter gene assays used for high-throughput screening. Chem. Res. Toxicol. 32, 1646–1655. https://doi.org/10.1021/acs.chemrestox.9b00182.

Fischer, F., Henneberger, L., König, M., Bittermann, K., Linden, L., Goss, K.-U., Escher, B., 2017. Modeling exposure in the Tox21 in vitro bioassays. Chem. Res. Toxicol. 30, 1197–1208. https://doi.org/10.1021/acs.chemrestox.7b00023.

Fischer, F.C., Henneberger, L., Schlichting, R., Escher, B.I., 2019. How to improve the dosing of chemicals in high-throughput in vitro mammalian cell assays. Chem. Res. Toxicol. 1462–1468. https://doi.org/10.1021/acs.chemrestox.9b00167.

Fitzsimmons, P.N., Fernandez, J.D., Hoffman, A.D., Butterworth, B.C., Nichols, J.W., 2001. Branchial elimination of superhydrophobic organic compounds by rainbow trout (*Oncorhynchus mykiss*). Aquat. Toxicol. 55, 23–34. https://doi.org/10.1016/

s0166-445x(01)00174-6.
Fujino, R., Hashizume, K., Aoyama, S., Maeda, K., Ito, K., Toshimoto, K., Lee, W., Ninomiya, S., Sugiyama, Y., 2018. Strategies to improve the prediction accuracy of hepatic intrinsic clearance of three antidiabetic drugs: application of the extended clearance concept and consideration of the effect of albumin on CYP2C metabolism and OATP1B-mediated hepatic uptake. Eur. J. Pharm. Sci. 125, 181–192. https://doi.org/10.1016/j.ejps.2018.09.021.
Gülden, M., Seibert, H., 2005. Impact of bioavailability on the correlation between in vitro cytotoxic and in vivo acute fish toxic concentrations of chemicals. Aquat. Toxicol. 72, 327–337. https://doi.org/10.1016/j.aquatox.2005.02.002.
Han, X., Nabb, D.L., Mingoia, R.T., Yang, C.H., 2007. Determination of xenobiotic intrinsic clearance in freshly isolated hepatocytes from rainbow trout (*Oncorhynchus mykiss*) and rat and its application in bioaccumulation assessment. Environ. Sci. Technol. 41, 3269–3276. https://doi.org/10.1021/es0626279.
Henneberger, L., Mühlenbrink, M., König, M., Schlichting, R., Fischer, F.C., Escher, B.I., 2019. Quantification of freely dissolved effect concentrations in in vitro cell-based bioassays. Arch. Toxicol. 93, 2295–2305. https://doi.org/10.1007/s00204-019-02498-3.
Heringa, M.B., Schreurs, R.H.M.M., Busser, F., Van Der Saag, P.T., Van Der Burg, B., Hermens, J.L.M., 2004. Toward more useful in vitro toxicity data with measured free concentrations. Environ. Sci. Technol. 38, 6263–6270. https://doi.org/10.1021/es049285w.
Hestermann, E.V., Stegeman, J.J., Hahn, M.E., 2000. Serum alters the uptake and relative potencies of halogenated aromatic hydrocarbons in cell culture bioassays. Toxicol. Sci. 53, 316–325. https://doi.org/10.1093/toxsci/53.2.316.
Jones, H.M., Houston, J.B., 2004. Substrate depletion approach for determining in vitro metabolic clearance: time dependencies in hepatocyte and microsomal incubations. Drug Metab. Dispos. 32, 973–982. https://doi.org/10.1124/dmd.104.000125.
Jonker, M.T.O., van der Heijden, S.A., 2007. Bioconcentration factor hydrophobicity cutoff: an artificial phenomenon reconstructed. Environ. Sci. Technol. 41, 7363–7369. https://doi.org/10.1021/es0709977.
Kim, S.-J., Lee, K.-R., Miyauchi, S., Sugiyama, Y., 2019. Extrapolation of in vivo hepatic clearance from in vitro uptake clearance by suspended human hepatocytes for anionic drugs with high binding to human albumin: improvement of in vitro-to-in vivo extrapolation by considering the “albumin-mediated” hepatic uptake mechanism on the basis of the “facilitated-dissociation model”. Drug Metab. Dispos. 47, 94–103. https://doi.org/10.1124/dmd.118.083733.
Kleinow, K.M., James, M.O., Tong, Z., Venugopalan, C.S., 1998. Bioavailability and biotransformation of benzo(*a*)pyrene in an isolated perfused in situ catfish intestinal preparation. Environ. Health Perspect. 106, 155–166. https://doi.org/10.1289/ehp.98106155.
Krause, S., Goss, K.-U., 2018a. In vitro-in vivo extrapolation of hepatic metabolism for different scenarios - a toolbox. Chem. Res. Toxicol. 31, 1195–1202. https://doi.org/10.1021/acs.chemrestox.8b00187.
Krause, S., Goss, K.-U., 2018b. The impact of desorption kinetics from albumin on hepatic extraction efficiency and hepatic clearance: a model study. Arch. Toxicol. 92, 2175–2182. https://doi.org/10.1007/s00204-018-2224-x.
Krause, S., Ulrich, N., Goss, K.-U., 2018. Desorption kinetics of organic chemicals from albumin. Arch. Toxicol. 92, 1065–1074. https://doi.org/10.1007/s00204-017-2117-4.
Kwon, J.-H., Katz, L.E., Liljestrand, H.M., 2007a. Modeling binding equilibrium in a competitive estrogen receptor binding assay. Chemosphere 69, 1025–1031. https://doi.org/10.1016/j.chemosphere.2007.04.047.
Kwon, J.-H., Wuethrich, T., Mayer, P., Escher, B.I., 2007b. Dynamic permeation method to determine partition coefficients of highly hydrophobic chemicals between poly (dimethylsiloxane) and water. Anal. Chem. 79, 6816–6822. https://doi.org/10.1021/ac0710073.
Kwon, J.-H., Wuethrich, T., Mayer, P., Escher, B.I., 2009. Development of a dynamic delivery method for in vitro bioassays. Chemosphere 76, 83–90. https://doi.org/10.1016/j.chemosphere.2009.02.023.
Lee, H.-J., Jung, J.-H., Kwon, J.-H., 2019. Evaluation of the bioaccumulation potential of selected alternative brominated flame retardants in marine fish using in vitro metabolic transformation rates. Sci. Total Environ. 653, 1333–1342. https://doi.org/10.1016/j.scitotenv.2018.10.432.
Lo, J.C., Allard, G.N., Otton, S.V., Campbell, D.A., Gobas, F.A.P.C., 2015. Concentration dependence of biotransformation in fish liver S9: optimizing substrate concentrations to estimate hepatic clearance for bioaccumulation assessment. Environ. Toxicol. Chem. 34, 2782–2790. https://doi.org/10.1002/etc.3117.
Lo, J.C., Letinski, D.J., Parkerton, T.F., Campbell, D.A., Gobas, F.A.P.C., 2016. In vivo biotransformation rates of organic chemicals in fish: relationship with bioconcentration and biomagnification factors. Environ. Sci. Technol. 50, 13299–13308. https://doi.org/10.1021/acs.est.6b03602.
Matsunaga, N., Ufuk, A., Morse, B.L., Bedwell, D.W., Bao, J., Mohutsky, M.A., Hillgren, K.M., Hall, S.D., Houston, J.B., Galetin, A., 2019. Hepatic OATP-mediated clearance in the Beagle dog: assessing in vitro-in vivo relationships and applying cross species empirical scaling factors to improve prediction of human clearance. Drug Metab. Dispos. 47, 215–226. https://doi.org/10.1124/dmd.118.084194.
Miyauchi, S., Masuda, M., Kim, S.J., Tanaka, Y., Lee, K.R., Iwakado, S., Nemoto, M., Sasaki, S., Shimono, K., Tanaka, Y., Sugiyama, Y., 2018. The phenomenon of albumin-mediated hepatic uptake of organic anion transport polypeptide substrates: prediction of the in vivo uptake clearance from the in vitro uptake by isolated hepatocytes using a facilitated-dissociation model. Drug Metab. Dispos. 46, 259–267. https://doi.org/10.1124/dmd.117.077115.
Nichols, J.W., Schultz, I.R., Fitzsimmons, P.N., 2006. In vitro-in vivo extrapolation of quantitative hepatic biotransformation data for fish - I. a review of methods, and strategies for incorporating intrinsic clearance estimates into chemical kinetic models. Aquat. Toxicol. 78, 74–90. https://doi.org/10.1016/j.aquatox.2006.01.017.
Nichols, J.W., Ladd, M.A., Fitzsimmons, P.N., 2018. Measurement of kinetic parameters for biotransformation of polycyclic aromatic hydrocarbons by trout liver S9 fractions: implications for bioaccumulation assessment. Appl. In Vitro Toxicol. 4, 365–378. https://doi.org/10.1089/aivt.2017.0005.
Poulin, P., Burczynski, F.J., Haddad, S., 2016. The role of extracellular binding proteins in the cellular uptake of drugs: impact on quantitative in vitro-to-in vivo extrapolations of toxicity and efficacy in physiologically based pharmacokinetic-pharmacodynamic research. J. Pharm. Sci. 105, 497–508. https://doi.org/10.1002/jps.24571.
Sangster, J., 1989. Octanol-water partition coefficients of simple organic compounds. J. Phys. Chem. Ref. Data 18, 1111–1228. https://doi.org/10.1063/1.555833.
Saunders, L.J., Fontanay, S., Nichols, J.W., Gobas, F.A.P.C., 2019. Concentration dependence of in vitro biotransformation rates of hydrophobic organic sunscreen agents in rainbow trout S9 fractions: implications for bioaccumulation assessment. Environ. Toxicol. Chem. 38, 548–560. https://doi.org/10.1002/etc.4342.
Schlautman, M.A., Morgan, J.J., 1993. Effects of aqueous chemistry on the binding of polycyclic aromatic hydrocarbons by dissolved humic materials. Environ. Sci. Technol. 27, 961–969. https://doi.org/10.1021/es00042a020.
Shimura, K., Murayama, N., Tanaka, S., Onozeki, S., Yamazaki, H., 2019. Suitable albumin concentrations for enhanced drug oxidation activities mediated by human liver microsomal cytochrome P450 2C9 and other forms predicted with unbound fractions and partition/distribution coefficients of model substrates. Xenobiotica 49, 557–562. https://doi.org/10.1080/00498254.2018.1482576.
Ter Laak, T.L., Durjava, M., Struijs, J., Hermens, J.L.M., 2005. Solid phase dosing and sampling technique to determine partition coefficients of hydrophobic chemicals in complex matrixes. Environ. Sci. Technol. 39, 3736–3742. https://doi.org/10.1021/es048406p.